ACS OMEGA

Open Access

http://pubs.acs.org/journal/acsodf

Article

Preparation of Baicalin Liposomes Using Microfluidic Technology and Evaluation of Their Antitumor Activity by a Zebrafish Model

Yuhao Gu, Liqiang Jin, Li Wang, Xianzheng Ma, Mingfa Tian, Ammara Sohail, Jianchun Wang,* and Daijie Wang*

Cite This: *ACS Omega* 2024, 9, 41289−41300

Read Online

ACCESS | Metrics & More | Article Recommendations | Supporting Information

ABSTRACT: Baicalin (BCL), a well-known flavonoid molecule, has numerous therapeutic applications. However, its low water solubility and bioavailability limit its applicability. Microfluidics is a new method for liposome preparation that provides efficient and rapid control of the process, improving the stability and controllability. This study used microfluidic techniques to create baicalin liposomes (BCL-LPs), first screening for optimal total flow rates (TFR) and flow rate ratios (FRR), and then optimizing the phospholipid concentration, phospholipid-to-cholesterol ratio, and Tween-80 concentration using univariate and response surface methodology approaches. The study found that the ideal phospholipid content was 9.5%, the phospholipid-to-cholesterol ratio was 9:1 (*w*:*w*), and the Tween-80 concentration was 15%. BCL-LPs achieved 95.323% ± 0.481% encapsulation efficiency under the optimum circumstances. Characterization indicated that the BCL-LPs were spherical and uniform in size, with a mean diameter of 62.32 nm ± 0.42, a polydispersity index of 0.092 ± 0.009, and a zeta potential of −25.000 mV ± 0.216. *In vitro* experiments found that BCL-LPs had a better slow-release effect and stability than the BCL monomer. In zebrafish bioassays, BCL-LPs performed better than BCL monomer in terms of biological activity and bioavailability. The established method provided a feasible medicine delivery platform for BCL and could apply for the transport and encapsulation of more natural compounds, expanding the applications of drug delivery systems in healthcare and cancer therapies.

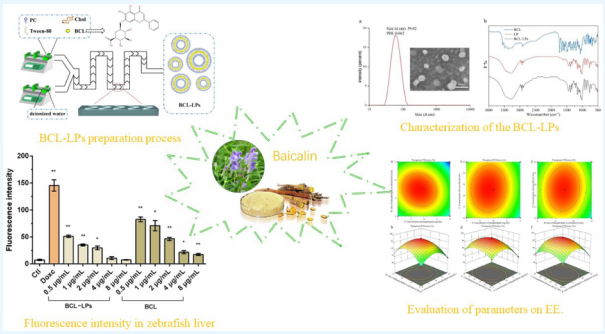

1. INTRODUCTION

A common drug in China is a flavonoid belonging to the glucuronic acid group called baicalin (BCL). It is taken out and separated from the dried root of the dicotyledonous Labiatae family plant, *Scutellaria baicalensis*.[1] Modern pharmacological studies have established that BCL has strong pharmacological activities, including antitumor,[2] anti-inflammatory,[3] antiviral,[4] and antibacterial effects.[5] Shi et al. discovered that BCL has a potential anticancer impact in liver cancer intervention by increasing NRF2/HO-1 expression and decreasing levels of NLRP3/Caspase1/GSDMD, which are engaged in the pyroptosis pathway.[6] Jiang et al. discovered that BCL could slow the progression of T2D-induced liver cancer by targeting epigenetic changes in the HKDC1 gene. It specifically modulates the m6A site (2854 site) *via* the METTL3 gene, indicating that it could be used to treat hepatic malignancies linked with diabetes.[7] However, BCL has been limited in medical applications due to its low water solubility and instability under physiological settings. Over the last two decades, nanodelivery of bioactive substances has emerged as a priority study area in food science. This is predicated on the benefits of nanoencapsulation and administration, such as improved stability and bioavailability of encapsulated compounds.[8] Therefore, various nanocarriers, including nanoliposomes,[9] nano emulsions,[10] microcapsules,[11] and hydrogels,[12] have been produced to encapsulate bioactive materials. The goal is to improve the stability, dispersion, bioavailability, and bioactive characteristics of phytochemicals for use as nano active carriers. Unlike other drug delivery technologies, liposomes can transport and preserve a wide range of hydrophilic and hydrophobic biomolecules. This is due to their unique phospholipid bilayer, which effectively protects the encapsulated bioactive chemicals from external influence.[13] Liposomes are made up of biocompatible materials that make them biodegradable and low in toxicity, increasing the solubility of the inserted medicine. They provide greater resistance to chemical and biological degradation during storage and administration in the human body.[14]

Received: April 9, 2024
Revised: September 3, 2024
Accepted: September 13, 2024
Published: September 24, 2024

Additional advantages include an increased therapeutic index and efficacy of medications encapsulated in liposomes as well as a reduction in direct exposure of sensitive tissues to hazardous chemicals. Because of their wide range of applications, several approaches for manufacturing and producing liposomes have emerged, including ether injection,[15] film dispersion,[16] reverse evaporation,[17] and freeze-drying methods.[18] However, throughout the production process, liposomes self-assemble in the phase volume, resulting in limited control and other uncontrolled aspects such as poor repeatability and low synthesis efficiency. Yulu Zhang et al., for example, developed borneol BCL liposomes with a maximum encapsulation efficiency of about 40%.[19] To address the aforementioned issues, liposome production can be optimized by using microfluidic technology. This approach enables fine control over the flow rates of the organic and aqueous phases, allowing for the creation of liposomes with adjustable sizes and improved encapsulation efficiency.[20]

The widespread usage of microfluidic technology highlights its immense potential in a variety of practical applications. Among these applications, the use of microfluidic technology in medication delivery has sparked increased interest and study.[21] Building on this, the size uniformity of liposomes can be achieved by microfluidic technology *via* precise regulation of parameters such as fluid flow rate and droplet size in microchannels, causing increased drug delivery stability and accuracy.[22] Following formulation screening, we wanted to identify baicalin-encapsulated liposome formulations with diameters under 100 nm and a low polydispersity index (PDI) that exhibit improved encapsulation rates. Nanoparticles less than 100 nm are often more effective for targeting tumors because their size allows for greater penetration. Those >100 nm are more likely to have poorer penetrating capabilities. Furthermore, nanoparticle size has a significant impact on their intracellular transport patterns, which might influence their accumulation in tumor tissues.[23]

The goal of this work was to use a microfluidic technique to efficiently and accurately create homogeneous BCL-LPs with high encapsulation efficiency, overcoming the limits of BCL's low water solubility and usage. First, response surface methodology (RSM) was used to construct and optimize the formulation of BCL-LPs, building on the increased bioavailability of BCL. We also evaluated liposomes manufactured using the optimal formulation in terms of *in vitro* release, salt, pH, heat, and storage stability. The results of the testing showed that in these various configurations, the BCL-LPs are quite stable. Then, experiments were performed on transgenic zebrafish strain *Tg (fabp10:rtTA2s-M2; TRE2:EGFP-kras^{V12})* to evaluate the effects of BCL and BCL-LPs on tumor cells.

2. MATERIAL AND METHODS

2.1. Materials. BCL (purity >98%) was purchased from Chengdu Desite Biological Technology Co., Ltd. (Chengdu, China). Soy lecithin was purchased from Shanghai Taiwei Pharmaceutical Co., Ltd. (Shanghai. China). Cholesterol was obtained from Shanghai Macklin Biochemical Technology Co., Ltd. (Shanghai, China). Mannitol was purchased from Beijing solarbio science and technology Co., Ltd. (Beijing, China). The anhydrous ethanol (HPLC grade, purity >99.9%) was obtained from China National Pharmaceutical Group Ltd. (Beijing, China). Phosphate-buffered saline (pH = 7.4) was purchased from Procell Life Science Co., Ltd. (Wuhan, China). In addition, the ultrapure water is used for liposome preparation.

2.2. Microfluidic Fabrication of BCL-LPs. Applying the technique described by Eman Jaradat,[24] we generated liposomes using a microfluidic apparatus. Using a 20-mL syringe, soy phospholipids, cholesterol, and Tween-80 were first dissolved in 15 mL of ethanol, according to the necessary ratios. A second 20-mL syringe was then filled with 15 mL of ultrapure water after that. Using a syringe pump, the ethanol and aqueous phases were fully mixed on a microfluidic liposome production chip to guarantee stable and homogeneous liposomes.[25]

2.3. Optimizing the Preparation Conditions of BCL-LPs. *2.3.1. Entrapment Efficiency of BCL-LPs.* First, we set up a BCL absorbance standard curve. After dissolving a suitable quantity of BCL in ethanol and diluting it according to predetermined ratios, the final concentrations are 20, 40, 60, 80, and 100 μg/mL. Next, we use a UV spectrophotometer to measure the absorbance at 278 nm and draw the standard curve (Figure S1).

We used the dialysis technique to calculate the encapsulation efficiency (EE) of the BCL-LPs. For disruption and subsequent centrifugation, 1 mL of liposomes was first combined with 3 mL of methanol and 6 mL of ultrapure water. A UV spectrophotometer (UV-1900) was used to measure the total drug content after the supernatant was collected. The next phase involved dialyzing 5 mL of liposomes for 12 h within a dialysis bag that had already been activated. The same method was used to test the absorbance of the resulting solution after dialysis. We determined the concentrations of free and total medicines by using the BCL absorbance standard curve. In the final step, the calculated value was obtained based on the given Equation 1.

$$\mathrm{EE}\% = \frac{C_{\mathrm{total}} - C_{\mathrm{free}}}{C_{\mathrm{total}}}^{*} 100\% \quad (1)$$

where C_{total} represents the total amount of BCL in liposome and C_{free} is the amount of free BCL in liposome.

2.3.2. Single Facts Experiment of BCL-LPs Preparation. The preliminary experiment revealed that the concentration of phospholipids, the ratio of phospholipids to cholesterol, and the content of Tween-80 are the most important parameters determining the encapsulation rate of BCL-LPs. The phospholipid concentration range was chosen from 6 to 14 mg/mL, the ratio of phospholipids to cholesterol from 3:1 to 15:1 (*w*:*w*), and the concentration of Tween-80 from 5 to 25 μL/mL. Each experiment included modifying one variable while keeping the others constant.

2.3.3. Optimization of BCL-LPs Preparative Condition by RSM. The preliminary experiment revealed that the concentration of phospholipids, the ratio of phospholipids to cholesterol, and the content of Tween-80 had the greatest impact on the encapsulation rate of BCL-LPs. As a result, 17 tests were carried out utilizing the Box−Behnken design (BBD) with the three specified components at three levels (3^3). Table 1 displayed the amounts and characteristics utilized in these tests. The F-test was employed to evaluate the statistical significance. In addition, the model's appropriateness was assessed by examining the coefficient of correlation (R^2), adjusted coefficient of determination (R^2_{adj}), and predicted coefficient of determination (R^2_{pred}). After choosing the most accurate model, the analysis of variance (ANOVA) was used to

https://doi.org/10.1021/acsomega.4c03356
ACS Omega 2024, 9, 41289−41300

Table 1. Levels and Code of Variables Chosen for Box−Behnken Design

Factors	code	Level and range		
		−1	0	1
Concentration of phospholipids (mg/mL)	A	8	10	12
Ratio of phospholipids to cholesterol (*w:w*)	B	6	9	12
Concentration of tween-80 (μL/mL)	C	10	15	20

examine the statistical significance of the regression coefficients.[26] Using Design-Expert Software, response surface graphs were generated. The optimum conditions were confirmed by conducting additional experiments under the mentioned conditions. A *p*-value of less than 0.05 represented statistical significance.

2.3.4. Characterization of BCL-LPs. The particle size, PDI, and potential of BCL-LPs were measured by using a dynamic light scattering instrument (Zetasizer Nano ZS90). Transmission electron microscopy (TEM) was also used to study the liposome morphology. For sample preparation, a suitable amount of a BCL-LPs solution was applied to the surface of a carbon-sprayed copper mesh and subsequently deposited. The sample was then colored with 2% phosphotungstic acid for 3 min. After natural drying, the morphology of BCL-LPs was examined using high-resolution TEM.

Fourier transform infrared spectroscopy (PerkinElmer) was used to confirm the interaction of BCL with liposomes. To preserve the liposomal structure, the sample was combined with a 10% mannitol solution, which served as a drying protectant. Following that, the mixture was freeze-dried and the resultant sample was transferred to a sample flask for examination. FT-IR spectra were acquired using a Vertex 70 FTIR spectrometer (Germany), encompassing the range from 4000 to 500 cm^{-1} with a resolution of 4 cm^{-1} while using a KBr pellet.

2.4. Methods for *In Vitro* Release and Stability Assessment of Liposomes. *2.4.1. In Vitro Release Studies.* The dialysis technique[27] was used to measure BCL-LP release *in vitro*. Each sample was put in a dialysis bag with a 5 mL capacity. The dialysis bag was then immersed in 50 mL of ultrapure water on a magnetic stirrer set at a constant temperature of 25 °C in darkness. At predefined intervals, 1 mL of the release medium was removed and replaced with 1 mL of ultrapure water. To ensure accuracy, the drug concentration in the release medium was measured immediately using a UV spectrophotometer. These data made it easier to calculate the drug release percentage at predefined intervals, allowing for a more thorough evaluation of the BCL-LPs' release profile.

2.4.2. Salt Stability Assessment. In the study, blank liposomes and BCL-LPs were incubated in NaCl aqueous solutions of varying concentrations (0−800 mM) at 25 °C to test the ionic stability of the liposome samples for a duration of 2 h. The particle size, PDI, and zeta potential of the samples were measured.

2.4.3. pH Stability Analysis. To conduct pH stability tests, blank liposomes and BCL-LPs were incubated in citric acid−Na_2HPO_4 buffer solutions with a pH range of 5 to 8, at 25 °C. The pH solutions were then combined with an equal volume of liposome systems. Incubation lasted 2 h at 25 °C. The particle size, PDI, and zeta potential of the samples were subsequently analyzed.

2.4.4. Thermal Stability Evaluation. The thermal stability of BCL-LPs was assessed at 80 °C over a period of 1 h. Samples were collected at various time intervals (0, 15, 30, 45, 60 min) and then immediately placed in an ice−water bath. The retention rate (%) of BCL following different durations of heat treatment was determined.

2.4.5. Storage Stability. In this study, under light-protected conditions at 4 and 25 °C, we evaluated the stability of BCL-LPs by measuring the average particle size, PDI, and zeta potential at predetermined intervals. This assessment lasted for 30 days.

2.5. Analysis of the Effects of BCL-LPs on the Transgenic Zebrafish. *2.5.1. Animals.* The transgenic zebrafish strain *Tg (fabp10:rtTA2s-M2; TRE2:EGFP-kras^{V12})* was obtained by the Zebrafish Drug Screening Platform at the Institute of Biotechnology, Shandong Academy of Sciences.

2.5.2. Feeding and Spawning of Zebrafish. The transgenic zebrafish Tg strain (*fabp10:rtTA2s-M2; TRE2:EGFP-kras^{V12}*) was reared at 28.5 °C with a daily light/dark cycle of 14 h light and 10 h dark. All zebrafish were kept for a regular duration of 2 weeks, and those who did not ovulate during this time were chosen. Before spawning, female and male zebrafish were kept in a tank at a 1:1 ratio. To guarantee regulated breeding, females and men were separated overnight using a partition. The divider was removed the next morning, allowing the male and female zebrafish to spontaneously mate. After around 3 h, the eggs were gathered. These eggs were subsequently immersed in E3 fish water, which had precise amounts of 5 mM NaCl, 0.17 mM KCl, 0.33 mM $CaCl_2$, and 0.33 mM $MgSO_4$. After 10 h of incubation, 0.003% phenylthiourea was given to avoid black blotches in the zebrafish embryos.

2.5.3. Evaluation of In Vivo Antitumor Activity in Zebrafish. Over the last two decades, the zebrafish model has been useful for investigating human illnesses like as cancer.[28] We employed the transgenic zebrafish strain *Tg (fabp10:rtTA2s-M2; TRE2:EGFP-kras^{V12})* as a model organism, finding that, in comparison to BCL, BCL-LPs demonstrated significantly enhanced antitumor efficacy within the zebrafish system. A transgenic strain of zebrafish *Tg (fabp10:rtTA2s-M2; TRE2:EGFP-kras^{V12})* born at 3 dpf was selected and added to 24-well plates for culture with 10 fish per well and 2 mL of E3 fish water. The zebrafish were randomly assigned into blank group (Ctl), doxycycline hydrochloride group (Doxc), BCL-LPs group (BCL-LPs, 0.5, 1, 2, 4, 8 μg/mL, based on the concentration of baicalein in liposomes), and BCL group (BCL, 0.5, 1, 2, 4, 8 μg/mL). The Ctl group was given normal E3 fish water for rearing. The Doxc group was supplemented with doxycycline hydrochloride at a concentration of 20 μg/mL. The BCL-LPs group was given varied concentrations of BCL-LPs, whereas the BCL group got variable concentrations of BCL. All groups were incubated for 4 days, with daily changes of fresh fish water and pharmacological treatments. By day 8, all zebrafish had been sedated with tricaine, placed on plates containing methylcellulose, and photographed. The average fluorescence intensity of the zebrafish liver was determined using Image-J software.

2.6. Statistical Analysis. To guarantee the reproducibility of our experimental findings, we independently repeated each experiment at least three times. The data were provided as mean values with accompanying standard deviations (±SD) to offer a thorough understanding of observed variability within the studies. For the studies involving response surface design,

https://doi.org/10.1021/acsomega.4c03356
ACS Omega 2024, 9, 41289−41300

we used the trial version of Design-Expert software (ver. 8.0.6, State-Ease Inc., Minneapolis, MN, USA). This program permitted the use of complex statistical tests, such as Analysis of Variance (ANOVA), allowing us to precisely analyze the significance of the acquired data.

3. RESULTS AND DISCUSSION

3.1. Flow Rate Screening for Baicalin-Encapsulated Liposomes. Microfluidic methods were employed to produce liposomes (Figure 1), and Figure 2 illustrated the effects of varying flow rate ratios (FRR) and total flow rates (TFR) on liposome particle size and PDI. We discovered that there were very minor variations in particle size when the TFR was changed from 400 to 1900 μL/min, while the FRR was kept constant. This illustrates that liposome size and distribution are not significantly impacted by the absolute shear pressures between parallel laminar flows. We found that reducing the FRR while maintaining a stable TFR produced smaller liposomes. This effect is due to greater shear stress in the liposome formation region induced by a higher flow rate ratio of the aqueous phase to the alcohol phase, which results in smaller liposome diameters. Meanwhile, the PDI drops and subsequently increases, possibly due to increased shear stress resulting in more uniform liposome production. However, if a certain threshold is reached, further complicated fluid dynamics effects emerge, resulting in an enhanced PDI. These findings are consistent with the conclusions drawn by Andreas Jahn et al.[29] According to Figure 2, we selected a TFR of 900 μL/ml and an FRR of 3:1 (water phase: alcohol phase, v/v) for subsequent experiments.

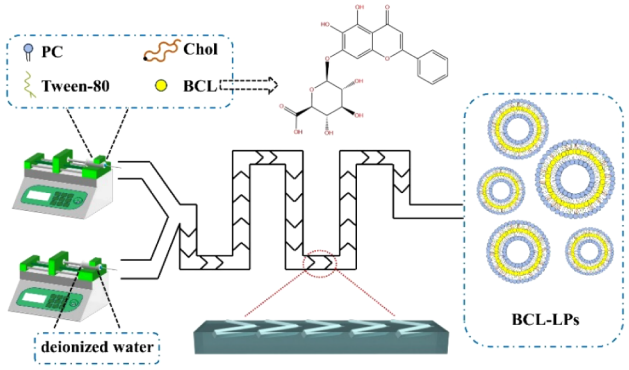

Figure 1. Graphic presentation of the BCL-LPs preparation process by chip.

3.2. Single Factor Experiment. *3.2.1. Effect of Phospholipid Concentration on BCL-LPs.* Several phospholipid concentrations (6, 8, 10, 12, and 14 mg/mL) were examined using a 9:1 (w:w) phospholipid-cholesterol ratio and a 15 μL/mL Tween-80 concentration. As shown in Figure 3 (a-b), the particle size of liposomes grew from 47.3 to 86.3 nm when the phospholipid concentration rose from 6 to 14 mg/mL. Encapsulation efficiency (EE) originally improved from 83.47% to 95.17%, but then declined to 81.17% as phospholipid content increased. This can be due to increased interaction between liposomes when phospholipid concentration rises, resulting in bigger particle sizes and an initial rise in EE.[30]

Based on Figure 3a,b, we decided to keep the phospholipid content at 10 mg/mL for the next single factor studies.

3.2.2. Effect of Phospholipid to Cholesterol Ratio on BCL-Lps. Using a phospholipid concentration of 10 mg/mL and a Tween-80 concentration of 15 μL/mL, the phospholipid-to-cholesterol ratio was calculated as 3:1, 6:1, 9:1, 12:1, and 15:1 (w:w).

As demonstrated in Figure 3c,d, when the phospholipid-to-cholesterol ratio grew from 3:1 to 15:1 (w:w), liposome encapsulation efficiency (EE) improved from 86.33% to

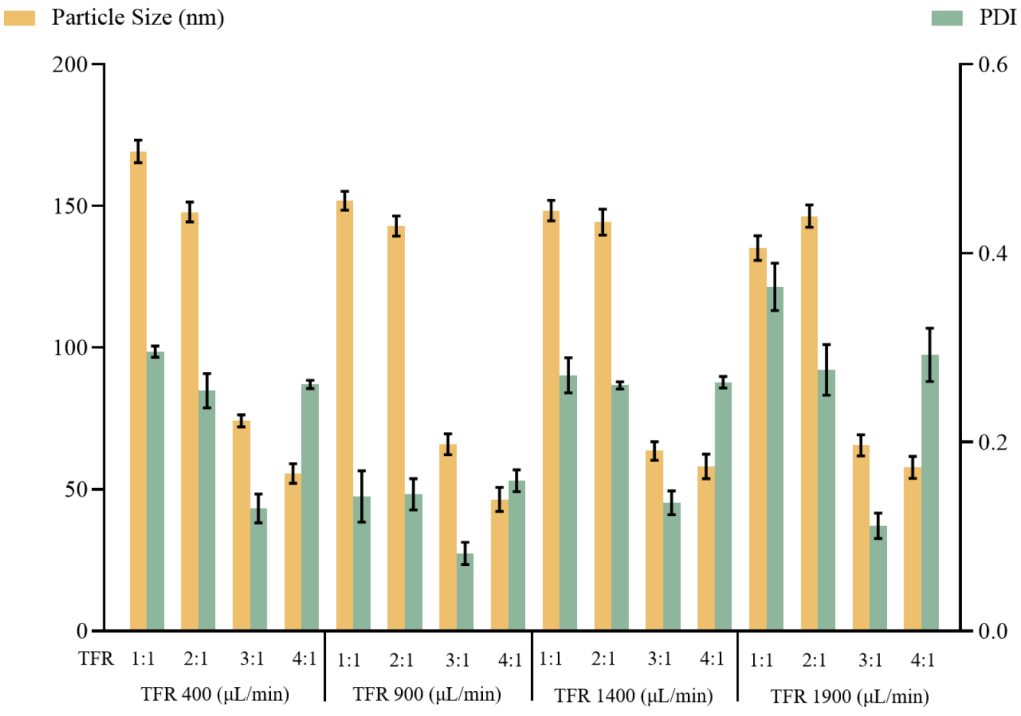

Figure 2. Effect of total flow rates and flow rate ratios on the liposome particle size and PDI.

https://doi.org/10.1021/acsomega.4c03356
ACS Omega 2024, 9, 41289−41300

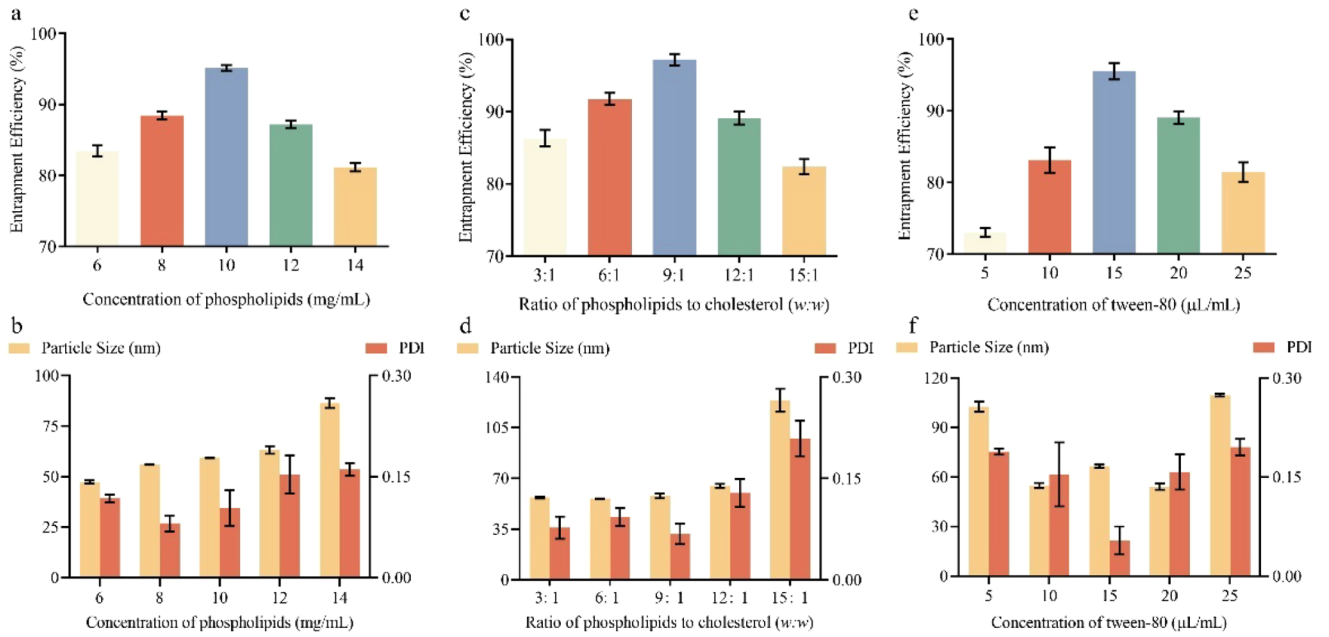

Figure 3. Effect of a single factor on the size, PDI, and EE of BCL-LPs. a and b: effects of phospholipids concentration; c and d: effects of phospholipids to cholesterol ratio; e and f: effects of tween-80 concentration. n = 5 for each group.

Table 2. Design and Results of Box–Behnken Experiments n = 5 for each group

	Levels of independent factors			Response: EE(%)	
No.	A	B	C	Predicted acquired EE	Practical acquired EE
1	10	9	15	94.85	95.13 ± 0.33
2	10	12	10	70.30	70.17 ± 0.05
3	10	6	20	74.13	74.26 ± 0.35
4	8	9	10	80.01	80.20 ± 0.49
5	8	6	15	71.74	71.90 ± 0.36
6	10	9	15	94.85	94.80 ± 0.08
7	12	6	15	67.71	67.77 ± 0.26
8	8	12	15	74.56	74.50 ± 0.69
9	10	9	15	94.85	95.70 ± 0.85
10	10	12	20	75.05	75.40 ± 0.43
11	10	6	10	75.22	74.87 ± 0.52
12	10	9	15	94.85	94.10 ± 0.16
13	10	9	15	94.85	94.53 ± 0.47
14	12	9	10	69.04	69.33 ± 0.49
15	8	9	20	79.72	79.43 ± 0.45
16	12	9	20	72.99	72.80 ± 0.43
17	12	12	15	60.90	60.74 ± 0.57

97.20% but subsequently decreased to 82.40% as the phospholipid-to-cholesterol ratio increased further. This can be due to cholesterol's positive influence on the denser arrangement of phospholipid molecules, which improves their ordering within liposomes. Nonetheless, when the cholesterol ratio in the phospholipid bilayer becomes very high or low, it produces a loss in compactness and, thus, a decline in EE.[31]

Based on the findings reported in Figure 3c,d, we chose to keep the phospholipid to cholesterol ratio at 9:1 (w:w) for the remaining single-factor trials.

3.2.3. Effect of Tween-80 Concentration on BCL-LPs. With other factors set at a phospholipid concentration of 10 mg/mL and a phospholipid-cholesterol ratio of 9:1 (w:w), the concentrations of tween-80 were 5, 10, 15, 20, and 25 μL/mL, respectively. The encapsulation efficiency (EE) of liposomes rose from 73.07% to 95.53% when the concentration of Tween-80 increased from 5 to 15 μL/mL, as shown in Figure 3e,f. However, the EE dropped to 81.47% when the concentration was increased to 25 μL/mL. This is explained by the intricate interplay between the generation of mixed micelles and the surfactant-induced instability of the liposome membrane, which lowers EE at greater Tween-80 concentrations.[32]

As presented in Figure 3ef, we fixed the concentration of tween-80 at 15 μL/mL for the subsequent single factor experiments.

3.3. Statistical Analysis and Model Fitting. The concentration of phospholipids, the ratio of phospholipids to cholesterol, and the concentration of Tween-80 were identified as important determinants in liposome production in this study (Table 1). The models were evaluated to exhibit changes in the encapsulation efficiency (EE).

The impacts of three parameters, namely, phospholipid concentration, phospholipid-to-cholesterol ratio, and Tween-80 concentration, were combined and tested on encapsulation efficiency (EE) at three levels. Table 2 shows the findings, and a 17-run BBD was used to optimize the parameters. The proposed fitted eq (Eq 2) may successfully predict the maximum EE and optimize the formula of BCL-LPs, as follows:

$$Y = 94.85 - 4.42A - 0.9988B + 0.9150C - 2.41AB + 1.06AC + 1.46BC - 12.18A^2 - 13.94B^2 - 7.23C^2 \quad (2)$$

Based on Table 3, the strength of the effects of the various influencing factors is A > B > C. The lack of fit associated with P-values of 0.69, demonstrated a no significance, supporting that the model fits with the data. In addition, with a high F-value, the proposed model effectively describes and forecasts the experimental outcomes,[33] as demonstrated by the

https://doi.org/10.1021/acsomega.4c03356
ACS Omega 2024, 9, 41289−41300

Table 3. ANOVA for Response Surface Quadratic Model[a]

Source	Sum of Squares	df	Mean Square	*F*-value	*p*-value	Prob > *F*
Model	2049.68	9	227.74	780.43	<0.0001	significant
A	156.56	1	156.56	536.49	<0.0001	
B	7.98	1	7.98	27.35	0.0012	
C	6.70	1	6.70	22.95	0.0020	
AB	23.18	1	23.18	79.45	<0.0001	
AC	4.49	1	4.49	15.40	0.0057	
BC	8.53	1	8.53	29.22	0.0010	
A^2	624.62	1	624.62	2140.45	<0.0001	
B^2	818.76	1	818.76	2805.76	<0.0001	
C^2	220.23	1	220.23	754.70	<0.0001	
Residual	2.04	7	0.29			
Lack of Fit	0.57	3	0.19	0.5216	0.6901	not significant
Pure Error	1.47	4	0.37			
Cor Total	2051.72	16				

[a]R^2=0.9990, R^2adj = 0.9977, R^2pred = 0.9944.

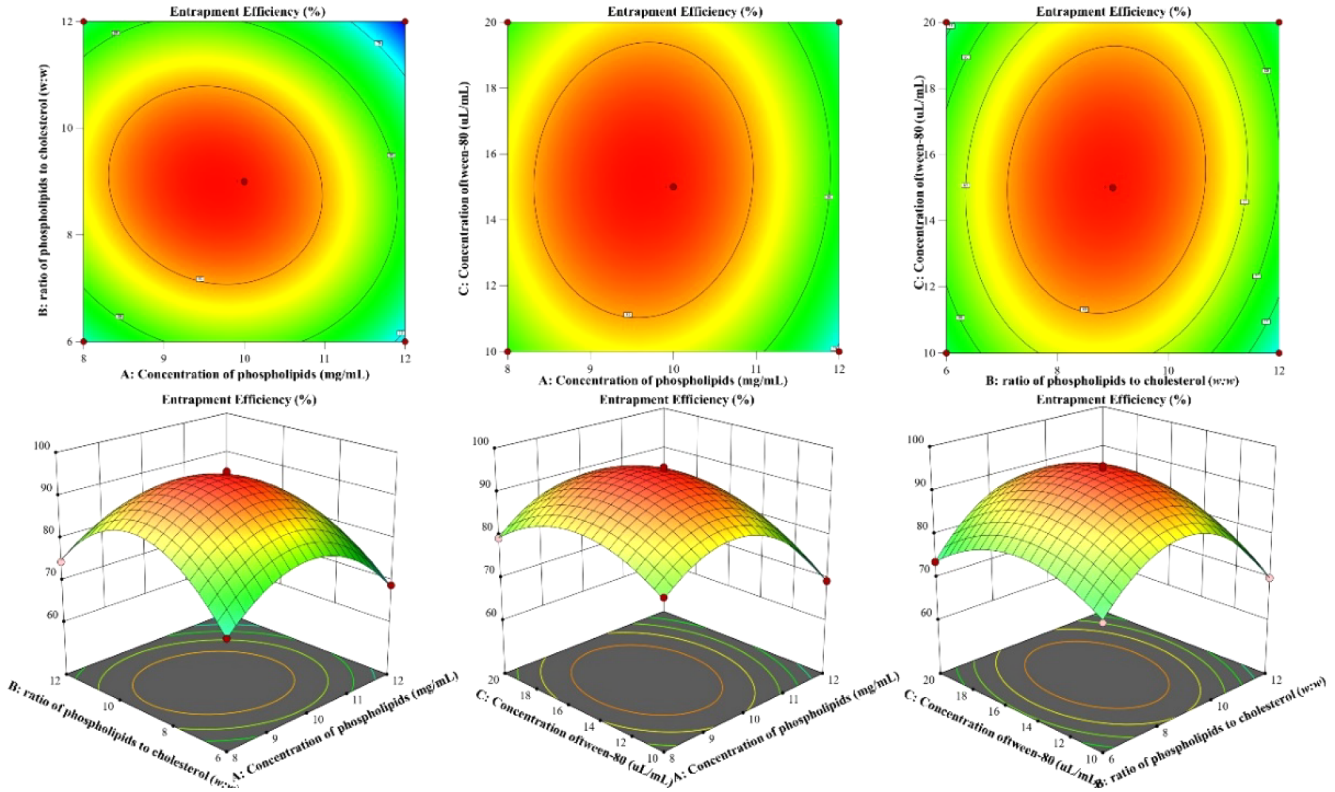

Figure 4. 3D response surface plots and 2D contour plots showing the effects of various parameters on EE.

Table 4. Predicted and Experimental Values of the Responses at Optimum Conditions

Factors and responses	Optimum conditions	Modified conditions
A: Concentration of phospholipids (mg/mL)	9.64	9.5
B: Ratio of phospholipids to cholesterol (*w*:*w*)	8.95	9.0
C: Concentration of tween-80 (μL/mL)	15.24	15.0
Encapsulation efficiency (%)	95.28	95.32 ± 0.48

correlation coefficient values of R^2=0.9990, R^2_{adj} = 0.9977, and R^2_{pred} = 0.9944.

The importance of the model terms was shown by their p-values, which were less than 0.01. The regression models were evaluated for their ability to explain response variability using the R^2 and R^2_{adj} values. Based on this information, we may infer that the model equation well predicts the encapsulation efficiency (EE%) in the current investigation.

3.4. Optimization of Preparation Conditions for BCL-LPs. The measured data were shown as 2D contour maps and 3D graphs by using the model polynomial function to assess changes in the response surface. These graphs also allowed for a deeper investigation of the link between the dependent and independent variables. As shown in Figures 4, 3D response surface and 2D contour maps were used to explain variable interactions and identify the best amounts of each variable under mutual impact in order to maximize response. The encapsulation effectiveness (EE%) of BCL-LPs varied between 60.74% and 95.70% depending on the phospholipid content,

https://doi.org/10.1021/acsomega.4c03356
ACS Omega 2024, 9, 41289−41300

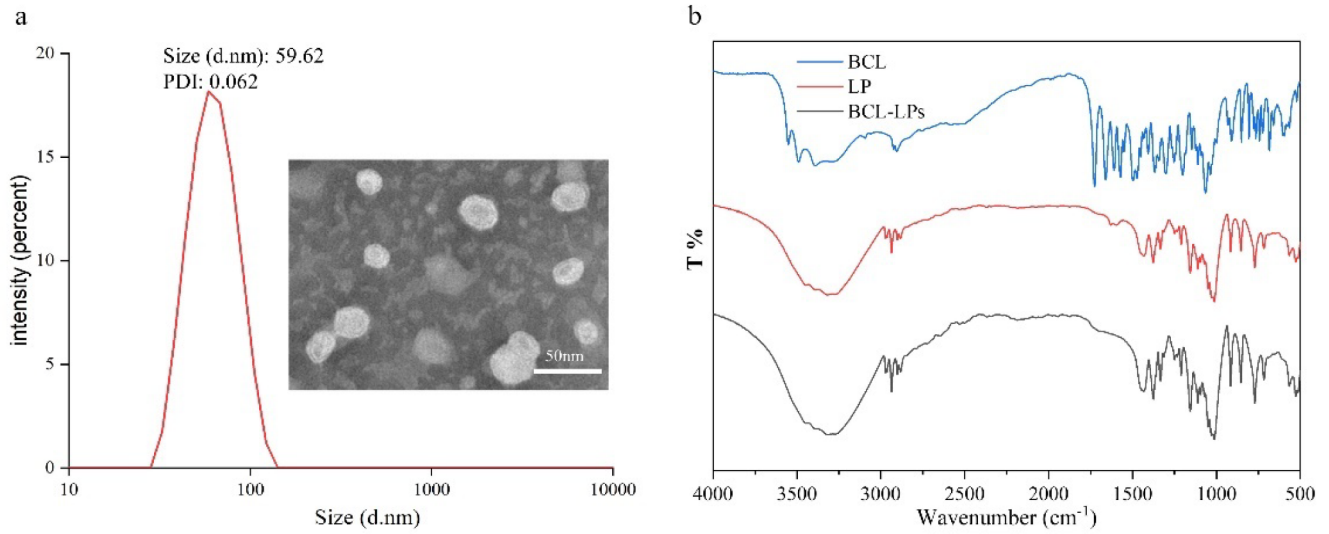

Figure 5. Characterization of the BCL-LPs. a: TEM images of BCL-LPs, b: FT-IR analysis of BCL, LPs, and BCL-LPs.

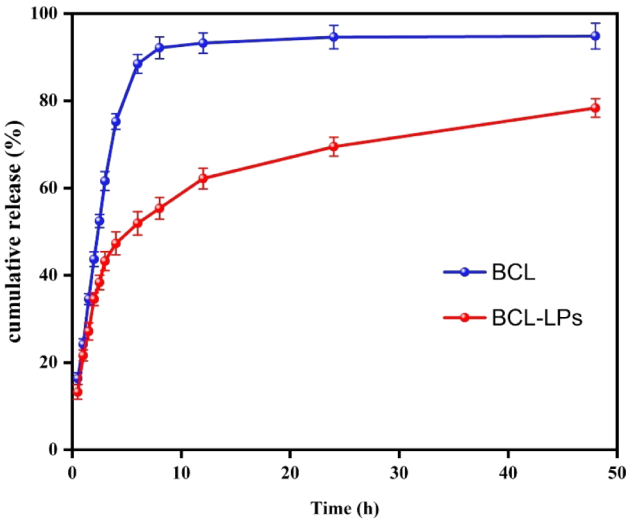

Figure 6. *In vitro* release simulations of BCL-LPs. n = 5 for each group.

phospholipid cholesterol ratio, Tween-80 concentration, and interactions (Figure 4).

EE% increases as each variable (phospholipid concentration, phospholipid-cholesterol ratio, and tween-80 concentration) increases and subsequently starts to decrease after reaching the maximum value. The maximum EE% was found to be in the following ranges: at around 9.64 mg/mL for phospholipid concentration, around 8.95:1 (w:w) for phospholipid-cholesterol ratio, and around 15.24 μL/mL for tween-80 concentration.

3.5. Validation of RSM Predictions. In Table 4, the Design Expert 8.0.6 software was used to predict optimal phospholipid concentrations of 9.64 mg/mL, a phospholipid-to-cholesterol ratio of 8.95:1 (w:w), and a Tween-80 concentration of 15.24 μL/mL during the liposome preparation process based on response surface graphs and analysis of variance. Under the parameters described above, the theoretical maximum encapsulation effectiveness (EE%) of BCL-LPs found to be 95.28%.

Three verification tests were conducted to ensure that the model equation was sufficient. The best parameters for preparing BCL-LPs in production practice are a phospholipid concentration of 9.5 mg/mL, a phospholipid-to-cholesterol ratio of 9:1 (w:w), and a Tween-80 concentration of 15.0 μL/mL. Under these circumstances, the encapsulation efficiency (EE%) of the BCL-LPs was 95.32 ± 0.48% ($n \geq 3$), matching the projected value. BCL-LPs had an average particle size of 62.320 ± 0.421 nm, PDI of 0.092 ± 0.009, and zeta potential of −25.000 ± 0.216 mV. This result validates the model and completely represents the predicted optimization and ensures that the model in eq 2 was accurate and reliable.

In our experimental design, we used the encapsulation efficiency (EE) as the key assessment parameter to examine the influence of all components. This choice was made with the purpose of creating a final liposome product with a high EE, tiny particle size, and low polydispersity index (PDI). These qualities are critical for assuring liposome stability, which is necessary for their efficacy and dependability in possible therapeutic applications.[34]

3.6. Characterization of Liposomes. *3.6.1. TEM Analysis.* As shown in Figure 5a, TEM images revealed that BCL-LPs were spherical in form with smooth surfaces and were around 50 nm. BCL-LPs showed vesicle-like structures, which was consistent with earlier liposomal formulation investigations.

3.6.2. FTIR Analysis. As demonstrated in Figure 5b, FT-IR analysis was carried out on freeze-dried powders of BCL, LPs, and BCL-LPs combined with spectroscopic grade KBr. The wavenumber range of 500−4000 cm^{-1} was scanned. The typical infrared peaks of BCL vanished in the BCL-LPs spectra, which consisted mostly of C═O and −COOH peaks. Furthermore, no additional peaks appeared, suggesting that BCL was confined within the self-assembled liposomes.

3.7. *In Vitro* Release and Stability Assessment of Liposomes. *3.7.1. In Vitro Release Study.* As the role of various forces between target drugs and liposomes, also the role of the liposomal bilayer, the release rate of drugs in liposomes could be significantly influence compared with the free drugs, thereby achieving a beneficial sustained-release capability.[35] Figure 6 shows the *in vitro* release characteristics between baicalin liposomes and monomer. BCL monomer showed an exponential increase, and the release rate reached 92.16% at 8 h, which indicated there was no slow-release effect.

https://doi.org/10.1021/acsomega.4c03356
ACS Omega 2024, 9, 41289−41300

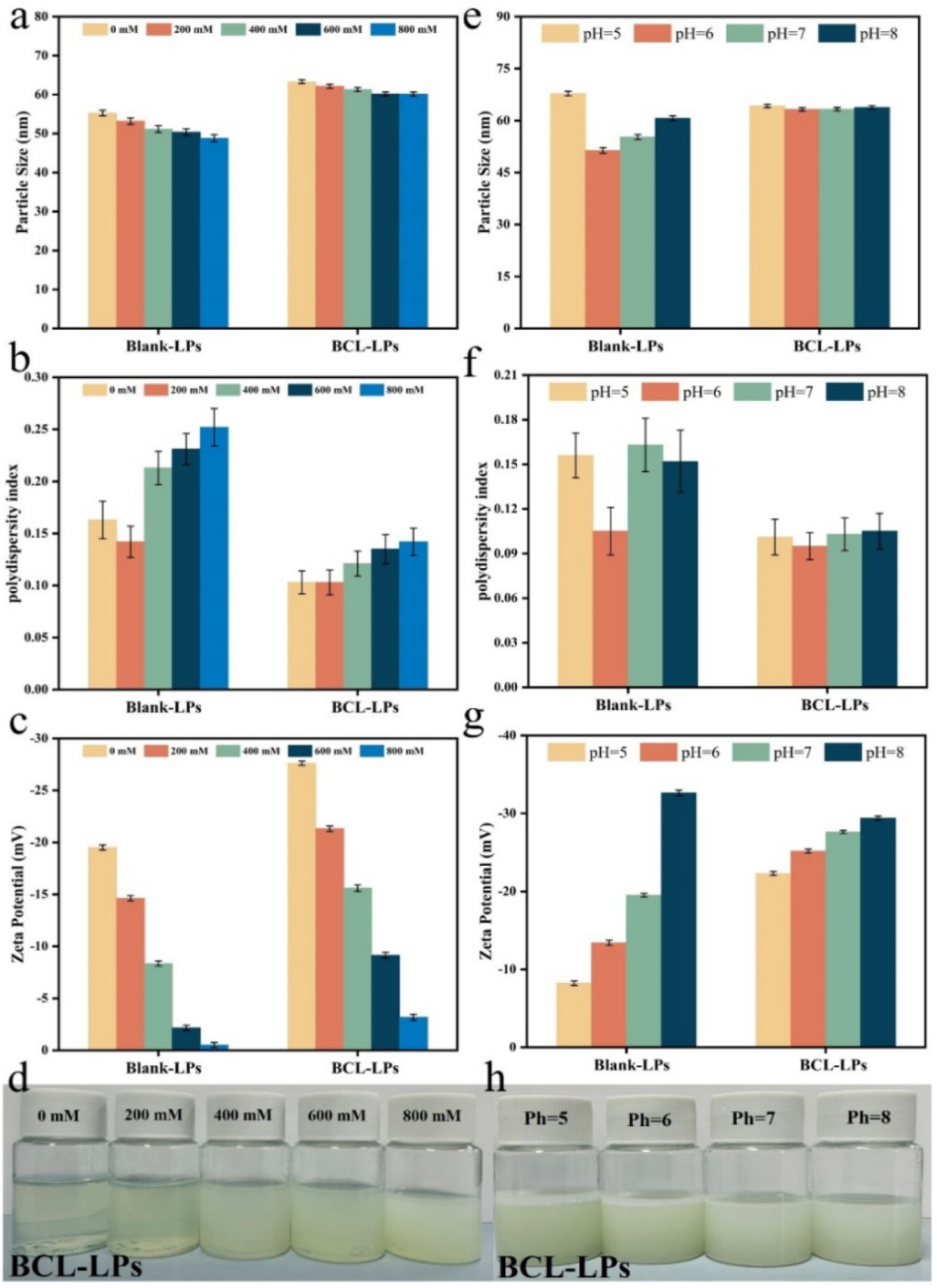

Figure 7. Effects of pH on particle size (a), PDI (b), zeta potential (c), and appearance (d). Effects of ionic strength on particle size (a), PDI (b), zeta potential (c), and appearance (d). n = 5 for each group.

However, the release rate of BC-LPs was only 55.36% at 8 h, significantly lower than that of the BCL monomer. At the time of 48 h, the release rate of BC-LPs was 78.36% and obviously lower than the BCL monomer of 94.85%. The results showed that encapsulating BCL within liposomes was not only enhanced its solubility in aqueous environments but also effectively controlled the release rate, thereby yielding a more prolonged release effect.[36]

Wu et al. investigated the *in vitro* release of astaxanthin monomer and liposomes. The results indicated that the astaxanthin liposomes were significantly lower than astaxanthin monomer within 10 h. The release rates of astaxanthin liposomes and monomer were approximately 40% and 90% at 48 h, suggesting an slow-release effect of liposomes.[37] Saroglu et al. investigated the *in vitro* release of crocin monomer and liposomes. The results demonstrated that the release of crocin monomer reached 95% at 9 h, whereas crocin liposomes exhibited slower release and reached only 48% at 27 h, significantly superior to crocin monomer.[38] The above results were consistent with the present results, which indicated that the prepared BC-LPs had the potential slow-release effect.

https://doi.org/10.1021/acsomega.4c03356
ACS Omega 2024, 9, 41289−41300

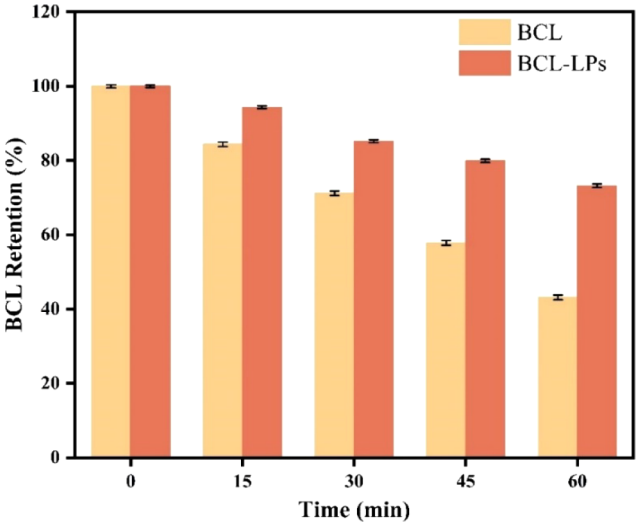

Figure 8. Thermal stability of the BCL-LPs. n = 5 for each group.

3.7.2. Salt Stability. For two h, equal amounts of Blank-LPs and BCL-LPs were combined with varying concentrations of NaCl solution (0−800 mM) and allowed to sit at room temperature. It was discovered that when the quantity of NaCl increased, the average particle size of both Blank-LPs and BCL-LPs decreased, as shown in Figure 7a. Blank-LPs' particle size dropped from 55.26 to 48.81 nm, whereas BCL-LPs' particle size dropped from 63.31 to 60.15 nm. This decrease is explained by osmotic processes, in which ions seep into the Nano liposomes' lipid bilayer and partially release water from inside.[39] Concurrently, as shown in Figure 7b, an increase in the PDI was observed for both Blank-LPs and BCL-LPs with an increasing NaCl concentration. Specifically, the PDI for Blank-LPs increased from 0.163 to 0.252, and for BCL-LPs, it rose from 0.103 to 0.142. This increase in PDI is attributed to the ions in NaCl shielding the surface charge of the liposomes, which reduces the electrostatic repulsion between them. This reduction in repulsion can lead to liposome aggregation or morphological changes, resulting in a broader distribution of particle sizes as indicated by the higher PDI values.[40] As illustrated in Figure 7c, the zeta potential of both Blank-LPs and BCL-LPs changed with increasing NaCl concentration, with Blank-LPs shifting from −19.51 to −0.51 mV and BCL-LPs shifting from −27.62 to −3.18 mV. This change is probably the result of interactions between the charged head groups on the liposome surface and the ions in the solution. The charge distribution is impacted by the increasing ionic strength, which changes the values of the zeta potential.[41] Compared with Blank-LPs, BCL-LPs exhibited stronger resistance to electrostatic charge shielding. The BCL-LPs solutions exhibited optical clarity throughout, as shown in Figure 7d, and not a single precipitation was noticed, even at an ionic strength of 800 mM.

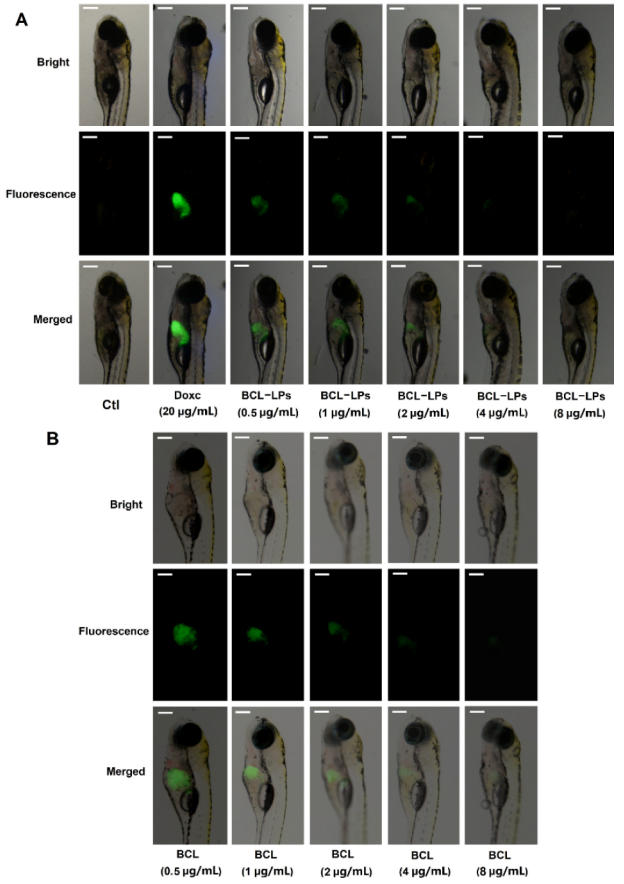

Figure 10. Treatment of zebrafish larvae with different concentrations of tested compounds induced an obvious fluorescence enhancement in the zebrafish liver. Scale bar is 200 μm. A: treated with Doxc (20 μg/mL), BCL-LPs (0.5, 1, 2, 4, and 8 μg/mL), B: treated with BCL (0.5, 1, 2, 4, and 8 μg/mL).

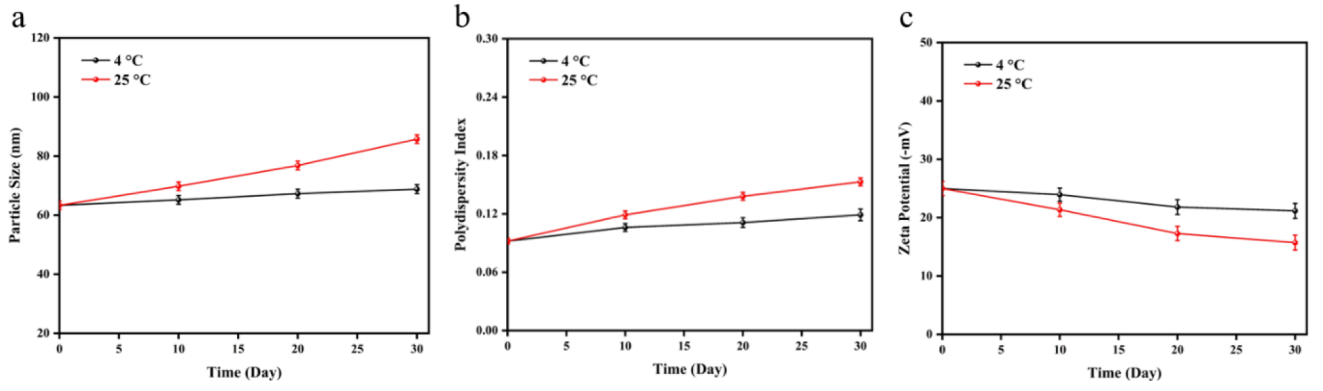

Figure 9. Storage stability of BCL-LPs at 4 and 25 °C for 30 days. a, b and c with the effects on particle size, polydispersity index, and zeta potential. n = 5 for each group.

https://doi.org/10.1021/acsomega.4c03356
ACS Omega 2024, 9, 41289−41300

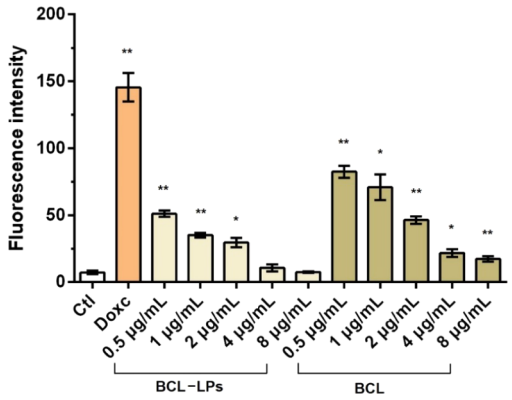

Figure 11. Fluorescence intensity in zebrafish liver after incubation with tested compounds and Doxc. Groups: Control (Ctl), BCL-LPs, BCL, Doxycycline Hyclate (Doxc). The data were analyzed by one-way ANOVA followed by Dunett's test using Graph Pad Prism 7.0 (GraphPad Software; CA, USA). $n = 5$ for each group. The results were expressed as mean ± SEM, $^{*}p < 0.05$, $^{**}p < 0.01$ VS Ctl.

3.7.3. pH Stability. The impact of different pH conditions on liposome systems is depicted in Figure 7e,f. The findings showed that pH variations had a major effect on the liposome systems. Significant size changes in Blank-LPs across various pH environments indicate instability within this pH range. BCL-LPs, on the other hand, perform substantially well; changes in size and appearance were minor between pH 5−8, showing relative stability under changing pH conditions. This stability is due to the hydrophobic contact between BCL and the liposomes' lipid bilayer. Such interactions provide a stable interface that limits the mobility of the phospholipid bilayer, boosting the overall stability of the liposomes.[42] As for appearance, as shown in Figure 7g, BCL-LP solutions maintain optical transparency with no significant precipitation observed in the pH range of 5−8.

3.7.4. Thermal Stability. Thermal stability studies were performed to assess the stability of liposomes at various temperatures, which is critical for establishing their suitability for storage and transportation. To determine the thermal stability of Nano liposomes, both BCL monomer and BCL-LPs were kept at 80 °C for 60 min. As shown in Figure 8, BCL monomer quickly escaped from the dialysis bag, leaving just 43.15% after 60 min. In contrast, the retention rate of BCL in BCL-LPs was greater than 73%, demonstrating that liposome encapsulation successfully preserves its stability under heat. This result is consistent with earlier investigations.[42]

3.7.5. Storage Stability. Figure 9 illustrates the storage stability of BCL-LPs at 4 and 25 °C over 30 days, measuring their average particle size, PDI, and zeta potential. As depicted in Figure 9a, at 4 °C, all samples exhibited a slight increase in size during storage, from 63.32 ± 0.421 nm to 68.82 ± 1.495 nm, whereas at 25 °C, BCL-LPs showed larger fluctuations, increasing to 85.75 ± 1.458 nm. Nanoliposomes are comparatively more stable at lower temperatures (4 °C) due to decreased membrane fluidity, whereas elevated temperatures may induce the breakage of ester bonds in phosphatidylcholine, leading to liposome aggregation. As demonstrated in Figure 9b, at 25 °C, the PDI of the samples increased significantly during storage compared to that at 4 °C, but remained below 0.2, indicating good dispersion of BCL-LPs at both temperatures. However, the PDI value at 25 °C is higher compared to 4 °C, further confirming the advantage of storing at 4 °C over 25 °C. In Figure 9c, it can be observed that compared to the condition at 25 °C, the absolute value change of BCL-LPs at 4 °C is minor, decreasing by only 3.84 mV. At the end of the 30-day storage period, the absolute value of zeta potential of BCL-LPs stored at 4 °C remains above 20 mV, indicating higher stability with a high surface charge, attributed to the electrostatic repulsion effect, maintaining their dispersion state.

3.8. Antitumor Activity of BCL-Lps in Zebrafish. As shown in Figure 10A, the blank group of transgenic line zebrafish *Tg (fabp10:rtTA2s-M2; TRE2:EGFP-kras^{V12})* exhibited no green fluorescence *in vivo*. The Doxc group expressed proto-oncogene kras^{v12} rapidly in the liver region under the stimulation of doxycycline hydrochloride and produced a strong green fluorescence. After supplementing different concentrations of BCL-LPs, the fluorescence in the liver region of zebrafish was significantly decreased, indicating that the expression of the proto-oncogene kras^{v12} was reduced, and the fluorescence intensity in the liver region gradually lowered with the gradual increase of BCL concentration in the liposomes (Figure 10A). When the concentration of BCL in liposomes reached 4 μg/mL, there was only a faint green fluorescence in the liver region. When the concentration reached 8 μg/mL, the fluorescence in the liver region disappeared. Compared to BCL-LPs, BCL inhibited the expression of the proto-oncogene kras^{v12} with average efficiency. BCL concentrations of 4 and 8 μg/mL resulted in modest green fluorescence in the liver area of zebrafish (Figure 10B), with a greater intensity compared to that of zebrafish treated with the same quantity of BCL-LPs (Figure 11).

4. CONCLUSION

In summary, a microfluidic technique was used in this work to quickly and effectively manufacture liposomes with high encapsulation efficiency. Optimal preparation conditions for BCL-LPs were identified by first screening the optimal FRR and TFR, then using RSM. These conditions included a phospholipid concentration of 9.5 mg/mL, a phospholipid to cholesterol ratio of 9:1 (*w:w*), and a Tween-80 concentration of 15 μL/mL. BCL-LPs demonstrated the following characteristics: a zeta potential of −25.000 ± 0.216 mV, an EE of 95.323 ± 0.481%, an average particle size of 62.320 ± 0.421 nm, and a PDI of 0.092 ± 0.009. Liposomes are characterized as tiny vesicles with a low PDI, highlighting their quality and consistency. The experimental results demonstrate BCL-LPs' outstanding sustained-release characteristics and stability. Furthermore, both BCL and BCL-LPs have excellent antitumor properties. However, BCL-loaded liposomes significantly inhibited the expression of the oncogene kras^{v12} in zebrafish, indicating a more potent antitumor action than BCL alone. These findings shed light on the circumstances and procedures used to prepare BCL-LPs, opening up possibilities for future study and development of cancer treatments. The established method could also be used in other natural products' liposomes with microfluidic technology. In the further study, the *in vivo* evaluation and toxicology studies of the prepared BCL-LPs would be researched.

■ ASSOCIATED CONTENT

Supporting Information

The Supporting Information is available free of charge at https://pubs.acs.org/doi/10.1021/acsomega.4c03356.

https://doi.org/10.1021/acsomega.4c03356
ACS Omega 2024, 9, 41289−41300

Validation of predictions (Particle Size, PDI); validation of predictions (zeta potential) and TEM image (PDF)

AUTHOR INFORMATION

Corresponding Authors

Jianchun Wang − *Shandong Giant E-Tech Co., Ltd., Jinan 250102, China*; Email: wangjianchun@outlook.com

Daijie Wang − *Heze Branch of Qilu University of Technology (Shandong Academy of Sciences), Heze 274000, China*; orcid.org/0000-0002-2156-4548; Email: wangdaijie@qlu.edu.cn

Authors

Yuhao Gu − *School of Light Industry Science and Engineering, Qilu University of Technology (Shandong Academy of Sciences), Jinan 250353, China; Heze Branch of Qilu University of Technology (Shandong Academy of Sciences), Heze 274000, China*

Liqiang Jin − *School of Light Industry Science and Engineering, Qilu University of Technology (Shandong Academy of Sciences), Jinan 250353, China*

Li Wang − *Jinan Vocational College of Engineering Department: Youth League Committee, Jinan 250200, China*

Xianzheng Ma − *Heze Branch of Qilu University of Technology (Shandong Academy of Sciences), Heze 274000, China*

Mingfa Tian − *Heze Branch of Qilu University of Technology (Shandong Academy of Sciences), Heze 274000, China*

Ammara Sohail − *University of Okara, Okara 56300, Pakistan*

Complete contact information is available at: https://pubs.acs.org/10.1021/acsomega.4c03356

Author Contributions

D.W. and Y.G. contributed to data curation; formal analysis, writing the original draft, and review and editing the manuscript. D.W. and J.W. contributed to conceptualization, funding acquisition, and review and editing the manuscript. X.M., M.T., and A.S. contributed to formal analysis and data curation. L.J. and L.W. contributed to data curation and writing the original draft. Y.G. contributed to formal analysis, investigation, and methodology.

Funding

This research received no external funding.

Notes

The authors declare no competing financial interest.

There were no any studies on human participants contained in this article. All applicable guidelines followed for the use and care of animals were institutional, national, and international. The zebrafish experiment was approved by the Animal Ethics Committee of the Biology Institute of Shandong Academy of Sciences (protocol no. SWS20230913).

ACKNOWLEDGMENTS

We gratefully acknowledge the Science, Education and Industry Integration Innovation Pilot Project from Qilu University of Technology (Shandong Academy of Sciences) (2022JBZ02-06, 2024ZDZX14), Key R&D Program of Shandong Province (2021CXGC010511, 2023TZXD068), the Science and Technology smes Innovation Ability Improvement Project of Shandong Province (2022TSGC2439), the Key R&D and transformation plan of Qinghai Province (2023-SF-112), Quancheng Industry Leading Talent Program and Quancheng "5150" Talent Introduction and Doubling Plan.

REFERENCES

(1) Wang, L.; Feng, T.; Su, Z.; Pi, C.; Wei, Y.; Zhao, L. Latest research progress on anticancer effect of baicalin and its aglycone baicalein. *Arch Pharm. Res.* **2022**, *45* (8), 535−557.

(2) Wang, B.; Huang, T.; Fang, Q.; Zhang, X.; Yuan, J.; Li, M.; Ge, H. Bone-protective and anti-tumor effect of baicalin in osteotropic breast cancer via induction of apoptosis. *Breast Cancer Res. Treat.* **2020**, *184* (3), 711−721.

(3) Xu, X.; Xia, J.; Zhao, S.; Wang, Q.; Ge, G.; Xu, F.; Liu, X.; Zhang, W.; Yang, Y. Qing-Fei-Pai-Du decoction and wogonoside exert anti-inflammatory action through down-regulating USP14 to promote the degradation of activating transcription factor 2. *Faseb J.* **2021**, *35* (9), No. e21870.

(4) Wei, Z.; Gao, R.; Sun, Z.; Yang, W.; He, Q.; Wang, C.; Zhang, J.; Zhang, X.; Guo, L.; Wang, S. Baicalin inhibits influenza A (H1N1)-induced pyroptosis of lung alveolar epithelial cells via caspase-3/GSDME pathway. *J. Med. Virol.* **2023**, *95* (5), No. e28790.

(5) Huang, Z.; Yu, Y.; Yang, H.-L.; Wang, Y.-F.; Huang, J.-L.; Xiao, L.; Liang, M.; Qi, J. Screening Antibacterial Constituents of Scutellaria Radix Based on Spectrum−Effect Relationships Between HPLC Fingerprints and the Inhibition of Oral Bacteria. *J. Chromatogr. Sci.* **2023**, *62* (1), 74−84.

(6) Shi, H.; Qiao, F.; Lu, W.; Huang, K.; Wen, Y.; Ye, L.; Chen, Y. Baicalin improved hepatic injury of NASH by regulating NRF2/HO-1/NRLP3 pathway. *Eur. J. Pharmacol.* **2022**, *934* (4), 175270.

(7) Jiang, H.; Yao, Q.; An, Y.; Fan, L.; Wang, J.; Li, H. Baicalin suppresses the progression of Type 2 diabetes-induced liver tumor through regulating METTL3/m(6)A/HKDC1 axis and downstream p-JAK2/STAT1/clevaged Capase3 pathway. *Phytomedicine* **2022**, *94* (1), 153823.

(8) Azzi, J.; Auezova, L.; Danjou, P.-E.; Fourmentin, S.; Greige-Gerges, H. First evaluation of drug-in-cyclodextrin-in-liposomes as an encapsulating system for nerolidol. *Food Chem.* **2018**, *255* (1), 399−404.

(9) Ding, Q.; Ding, C.; Liu, X.; Zheng, Y.; Zhao, Y.; Zhang, S.; Sun, S.; Peng, Z.; Liu, W. Preparation of nanocomposite membranes loaded with taxifolin liposome and its mechanism of wound healing in diabetic mice. *Int. J. Biol. Macromol.* **2023**, *241* (1), 124537−124541.

(10) Sessa, M.; Balestrieri, M. L.; Ferrari, G.; Servillo, L.; Castaldo, D.; D'Onofrio, N.; Donsì, F.; Tsao, R. Bioavailability of encapsulated resveratrol into nanoemulsion-based delivery systems. *Food Chem.* **2014**, *147* (1), 42−50.

(11) Huang, G.-Q.; Wang, H.-O.; Wang, F.-W.; Du, Y.-L.; Xiao, J.-X. Maillard reaction in protein − polysaccharide coacervated microcapsules and its effects on microcapsule properties. *Int. J. Biol. Macromol.* **2020**, *155* (1), 1194−1201.

(12) Asadi, N.; Pazoki-Toroudi, H.; Del Bakhshayesh, A. R.; Akbarzadeh, A.; Davaran, S.; Annabi, N. Multifunctional hydrogels for wound healing: Special focus on biomacromolecular based hydrogels. *Int. J. Biol. Macromol.* **2021**, *170* (1), 728−750.

(13) Bartelds, R.; Nematollahi, M. H.; Pols, T.; Stuart, M. C. A.; Pardakhty, A.; Asadikaram, G.; Poolman, B. Niosomes, an alternative for liposomal delivery. *PLoS One* **2018**, *13* (4), No. e0194179.

(14) Marto, J.; Vitor, C.; Guerreiro, A.; Severino, C.; Eleutério, C.; Ascenso, A.; Simões, S. Ethosomes for enhanced skin delivery of griseofulvin. *Colloids Surf., B* **2016**, *146* (1), 616−623.

(15) Du, B.; Li, Y.; Li, X.; Youmei, A.; Chen, C.; Zhang, Z. Preparation, characterization and in vivo evaluation of 2-methoxyestradiol-loaded liposomes. *Int. J. Pharm.* **2010**, *384* (1), 140−147.

(16) Lin, L.; Chen, W.; Li, C.; Cui, H. Enhancing stability of Eucalyptus citriodora essential oil by solid nanoliposomes encapsulation. *Ind. Crops Prod.* **2019**, *140* (1), 111615−111622.

(17) Liu, C.; Liu, Y.-Y.; Chang, Q.; Shu, Q.; Shen, N.; Wang, H.; Xie, Y.; Deng, X. Pressure-Controlled Encapsulation of Graphene Quantum Dots into Liposomes by the Reverse-Phase Evaporation Method. *Langmuir* **2021**, *37* (48), 14096−14104.

(18) Savadi, P.; Lotfipour, F.; McMillan, N. A. J.; Hashemzadeh, N.; Hallaj-Nezhadi, S. Passive and pH-gradient loading of doxycycline into nanoliposomes using modified freeze-drying of a monophase solution method for enhanced antibacterial activity. *Chem. Pap.* **2022**, *76* (5), 3097−3108.
(19) Zhang, Y.; Liu, S.; Wan, J.; Yang, Q.; Xiang, Y.; Ni, L.; Long, Y.; Cui, M.; Ci, Z.; Tang, D.; Li, N.; et al. Preparation, Characterization and in vivo Study of Borneol-Baicalin-Liposomes for Treatment of Cerebral Ischemia-Reperfusion Injury. *Int. J. Nanomed.* **2020**, *15* (5), 5977−5989.
(20) Lim, S. W. Z.; Wong, Y. S.; Czarny, B.; Venkatraman, S. Microfluidic-directed self-assembly of liposomes: Role of interdigitation. *J. Colloid Interface Sci.* **2020**, *578* (7), 47−57.
(21) Liu, Y.; Yang, G.; Hui, Y.; Ranaweera, S.; Zhao, C.-X. Microfluidic Nanoparticles for Drug Delivery. *Small* **2022**, *18* (36), 2106580.
(22) Feng, J.; Neuzil, J.; Manz, A.; Iliescu, C.; Neuzil, P. Microfluidic trends in drug screening and drug delivery. *TrAC, Trends Anal. Chem.* **2023**, *158* (1), 116821.
(23) Chen, Y.; Van Minh, L.; Liu, J.; Angelov, B.; Drechsler, M.; Garamus, V. M.; Willumeit-Römer, R.; Zou, A. Baicalin loaded in folate-PEG modified liposomes for enhanced stability and tumor targeting. *Colloids Surf., B* **2016**, *140* (1), 74−82.
(24) Jaradat, E.; Weaver, E.; Meziane, A.; Lamprou, D. A. Synthesis and Characterization of Paclitaxel-Loaded PEGylated Liposomes by the Microfluidics Method. *Mol. Pharmaceutics* **2023**, *20* (12), 6184−6196.
(25) Aranguren, A.; Torres, C. E.; Muñoz-Camargo, C.; Osma, J. F.; Cruz, J. C. Synthesis of Nanoscale Liposomes via Low-Cost Microfluidic Systems. *Micromachines* **2020**, *11* (12), 1050.
(26) Li, Z.; Lu, D.; Gao, X. Optimization of mixture proportions by statistical experimental design using response surface method - A review. *J. Build. Eng.* **2021**, *36* (1), 102101.
(27) Zhou, F.; Xu, T.; Zhao, Y.; Song, H.; Zhang, L.; Wu, X.; Lu, B. Chitosan-coated liposomes as delivery systems for improving the stability and oral bioavailability of acteoside. *Food Hydrocoll* **2018**, *83* (1), 17−24.
(28) McConnell, A. M.; Noonan, H. R.; Zon, L. I. Reeling in the Zebrafish Cancer Models. *Annu. Rev. Cancer Biol.* **2021**, *5* (1), 331−350.
(29) Andreas, J.; Vreeland, W. N.; DeVoe, D. L.; Locascio, L. E.; Michael, G. Microfluidic directed formation of liposomes of controlled size. *Langmuir* **2007**, *23* (11), 6289−6293.
(30) (a) Jin, H.-H.; Lu, Q.; Jiang, J.-G. Curcumin liposomes prepared with milk fat globule membrane phospholipids and soybean lecithin. *Int. J. Dairy Sci.* **2016**, *99* (3), 1780−1790. (b) Wu, Y.; Mou, B.; Song, S.; Tan, C.-P.; Lai, O.-M.; Shen, C.; Cheong, L.-Z. Curcumin-loaded liposomes prepared from bovine milk and krill phospholipids: Effects of chemical composition on storage stability, in-vitro digestibility and anti-hyperglycemic properties. *Int. Food Res. J.* **2020**, *136* (3), 109301.
(31) Lange, Y.; Steck, T. L. Cholesterol homeostasis and the escape tendency (activity) of plasma membrane cholesterol. *Prog. Lipid Res.* **2008**, *47* (5), 319−332.
(32) Nadzir, M. M.; Tan, W. F.; Mohamed, A. R.; Hisham, S. F. Size and Stability of Curcumin Niosomes from Combinations of Tween 80 and Span 80. *Sains Malays* **2017**, *46* (12), 2455−2460.
(33) Wu, Y.; Yi, L.; Li, E.; Li, Y.; Lu, Y.; Wang, P.; Zhou, H.; Liu, J.; Hu, Y.; Wang, D. Optimization of Glycyrrhiza polysaccharide liposome by response surface methodology and its immune activities. *Int. J. Biol. Macromol.* **2017**, *102* (1), 68−75.
(34) (a) Yun, J.-S.; Hwangbo, S.-A.; Jeong, Y.-G. Preparation of Uniform Nano Liposomes Using Focused Ultrasonic Technology. *Nanomaterials* **2023**, *13* (19), 2618. (b) Danaei, M.; Dehghankhold, M.; Ataei, S.; Davarani, F. H.; Javanmard, R.; Dokhani, A.; Khorasani, S.; Mozafari, M. R. Impact of Particle Size and Polydispersity Index on the Clinical Applications of Lipidic Nanocarrier Systems. *Pharmaceutics* **2018**, *10* (2), 57.
(35) Chen, L.; Lan, J.; Li, Z.; Zeng, R.; Wang, Y.; Zhen, L.; Jin, H.; Ding, Y.; Zhang, T. A Novel Diosgenin-Based Liposome Delivery System Combined with Doxorubicin for Liver Cancer Therapy. *Pharmaceutics* **2022**, *14* (8), 1685.
(36) Abbasi, H.; Kouchak, M.; Mirveis, Z.; Hajipour, F.; Khodarahmi, M.; Rahbar, N.; Handali, S. What We Need to Know about Liposomes as Drug Nanocarriers: An Updated Review. *Adv. Pharm. Bull* **2023**, *13* (1), 7−23.
(37) Wu, H.; Zhang, H.; Li, X.; Secundo, F.; Mao, X. Preparation and characterization of phosphatidyl-agar oligosaccharide liposomes for astaxanthin encapsulation. *Food Chem.* **2023**, *404*, 134601.
(38) Saroglu, O.; Atalı, B.; Yıldırım, R. M.; Karadag, A. Characterization of nanoliposomes loaded with saffron extract: in vitro digestion and release of crocin. *J. Food Meas. Charact.* **2022**, *16* (6), 4402−4415.
(39) Cheng, C.; Wu, Z.; McClements, D. J.; Zou, L.; Peng, S.; Zhou, W.; Liu, W. Improvement on stability, loading capacity and sustained release of rhamnolipids modified curcumin liposomes. *Colloids Surf., B* **2019**, *183* (1), 110460.
(40) Rahnfeld, L.; Thamm, J.; Steiniger, F.; van Hoogevest, P.; Luciani, P. Study on the in situ aggregation of liposomes with negatively charged phospholipids for use as injectable depot formulation. *Colloids Surf., B* **2018**, *168* (1), 10−17.
(41) Németh, Z.; Csóka, I.; Semnani Jazani, R.; Sipos, B.; Haspel, H.; Kozma, G.; Kónya, Z.; Dobó, D. G. Quality by Design-Driven Zeta Potential Optimisation Study of Liposomes with Charge Imparting Membrane Additives. *Int. J. Pharm.* **2022**, *14* (9), 1798.
(42) Li, R.; Pu, C.; Sun, Y.; Sun, Q.; Tang, W. Interaction between soybean oleosome-associated proteins and phospholipid bilayer and its influence on environmental stability of luteolin-loaded liposomes. *Food Hydrocoll* **2022**, *130* (1), 107721−107721.

https://doi.org/10.1021/acsomega.4c03356
ACS Omega 2024, 9, 41289−41300